ACTA IMEKO
ISSN: 2221-870X
June 2025, Volume 14, Number 2, 1 - 10

Laser line triangulation measurement on incandescent steel objects: methodologies to improve optical signal to noise ratio

Valentina Pasquinelli [1], Milena Martarelli[1], Luigi Montalto[2], Matteo Nisi[1], Helmert Van de Kamp[3], Bart Verhoef[3], Nicola Paone[1]

[1] *Dip. di Ingegneria Industriale e Scienze Matematiche (DIISM), Marche Polytechnic University, Via Brecce Bianche 12, 60131 Ancona, Italy*
[2] *Dip. di Scienze e Ingegneria della Materia, dell'Ambiente ed Urbanistica (SIMAU), Marche Polytechnic University, Via Brecce Bianche 12, 60131 Ancona, Italy*
[3] *VDL WEWELER bv, Ecofactorij 10, 7325WC Apeldoorn, The Netherlands*

ABSTRACT
Integrating optical sensors into harsh industrial environments poses challenges and limits to the application. This paper discusses the implementation of a LLT (Laser Line Triangulation) sensor in a steel industry use case, designed to measure the straightness of steel bars at very high temperatures, up to 1000-1200 °C. Due to the bar incandescence it is challenging to use the optical instrument, as Signal to Noise Ratio (SNR) of the laser line projected onto the inspected object is lower than 2 dB. Both hardware and software solutions are investigated, in particular the choice of a very narrowband filter is selected to remove quite all the other spectral content coming from the bar irradiance. Even though this solution enhances SNR, the narrow band filter blocks the laser irradiance at the edges of the field of view: a reference ruler measured at ambient temperature has shown that 40.3 % of the length of the bar is not detected with respect to the measurement without the narrow band filter. To cope with this issue, a software solution is implemented which consists in the preprocessing of the image with a Region of Interest (ROI) around the laser line. This solution imposes the constraint of repeatable product positioning which has to be assured by the robot which picks up the product for the measurement. Applying the ROI, the Laser Line Extraction (LLE) algorithm detects clearly the laser line, with outliers reduction of 97.5 % with respect to the case without ROI introduction.

Section: RESEARCH PAPER

Keywords: Laser line triangulation; interference filters; steel incandescence; signal to noise ratio; optical angle

Citation: V. Pasquinelli, M. Martarelli, L. Montalto, M. Nisi, H. Van de Kamp, B. Verhoef, N. Paone, Laser line triangulation measurement on incandescent steel objects: methodologies to improve optical signal to noise ratio, Acta IMEKO, vol. 14 (2025) no. 2, pp. 1-10. DOI: 10.21014/actaimeko.v14i2.2069

Section Editor: Andrea Scorza, University Roma Tre, Italy

Received February 3, 2025; **In final form** June 9, 2025; **Published** June 2025

Funding: This work was partially supported by OPENZDM project. This is a project from the European Union's Horizon Europe research and innovation program under Grant Agreement No. 101058673 in the call HORIZON-CL4-2021-TWIN-TRANSITION-01.

Corresponding author: Valentina Pasquinelli, e-mail: v.pasquinelli@pm.univpm.it

1. INTRODUCTION

Measuring on incandescent products is challenging when using optical sensors as irradiance coming from the product reduces SNR (Signal to Noise Ratio). This paper presents methodologies on how to improve SNR while using a Laser Line Triangulation (LLT) sensor on incandescent steel products. The application has been developed in the context of the openZDM project [1] which aims to install Non-Destructive Inspection (NDI) systems in production lines and integrate them to an open platform designed to implement a Zero-Defect Manufacturing (ZDM) approach. Defect prevention and prediction is fundamental for the reduction of product scrap and both environmental and economic impact of the production process. Different measurement techniques are reported in literature for non-contact product inspection in steel industry for example for welding or hot forging [2] such as vision-based systems [3], laser structuring systems [4], ultrasounds [5] and more. This paper exploits the Laser Line Triangulation (LLT) technique for geometry measurement presenting a LLT sensor installed in the

production line of VDLWEW b.v., which produces air suspension trailing arms, with the objective of measuring the straightness of steel bars being processed. The product is measured at very high temperatures up to 1000-1200 °C, which makes it necessary to implement a non-contact measurement method but challenging to use an optical instrument due to the bar incandescence. Hot parts at forging temperatures, typically 900–1300 °C, emit a considerable amount of energy in the infrared spectrum [6]. Indeed, the hot product can be approximated as a blackbody at 1200 °C. The product to be inspected is a steel bar which straightness has to be measured and controlled, in order to reduce defect propagation along the production line. Non-straight bars lead in fact to final non-conformity of the product as the defect enhances during the progressive steps of the process such as rolling or punching [7].

In literature, different geometry measurement techniques for high temperature objects based on LLT [8] and on spectral selective techniques [9] have been applied to hot forging. Moreover, research work by Määttä et al. show that time of flight (TOF) laser scanners are suitable for scanning hot surfaces [10], [11]. To enhance SNR, a hardware solution is to equip the camera with a filter centred at the laser wavelength [12], [13]. This solution is investigated also in this paper and its limits are highlighted as a very narrow band filter can remove too much the spectral content reaching the camera lens, not allowing to measure correctly at the edges of the field of view of the sensor. Also software solutions can be implemented, as the application of multi-step algorithms which include initial guesses that can help detecting the object of interest correctly. For example, in [14] the authors present a methodology for axis straightness measurement of hot forgings: a step of initial detection for the length of the forging is used, before the main detection algorithm, in order to limit the area of interest. This paper as well presents a software solution to enhance SNR ratio which is the preprocessing of the image with a Region of Interest so that the Laser Line Extraction algorithm performs correctly.

Section 2 describes the optical design of the LLT sensor with particular focus to the laser wavelength and the camera optical filters applied. Different filters are discussed and the feasibility of their introduction for the inline application is investigated. Section 3 describes the methodology to estimate and therefore improve SNR of the laser line extracted discussing the attenuation of the laser line signal with respect to the noise signal and the influence of the sensitivity to the optical angle. Section 4 reports the approach for the inline application presenting methodologies to optimize both acquisition parameters and laser line extraction algorithm. Finally, Section 5 reports the conclusions and future development of the work.

2. OPTICAL DESIGN OF THE LASER LINE TRIANGULATION SENSOR

The product to be inspected exits the steps of induction furnace and descaling unit and its temperature ranges between 1000-1200 °C. To evaluate the right wavelength for the laser to be used it is important to consider the spectral radiance of the hot steel bar and how it affects the signal reaching the camera sensor. This paragraph shows how to evaluate the appropriate laser line wavelength for the LLT sensor and describes the final prototype design.

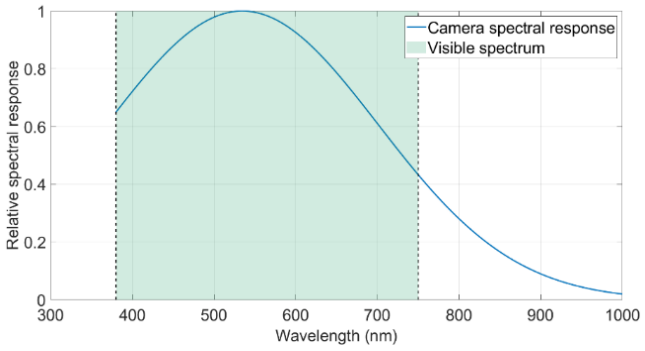

Figure 1. Camera spectral response, model AT C5-2040-GigE.

2.1. Laser Line Emitter Wavelength Selection

The LLT sensor features a monochrome camera, model AT C5-2040-GigE, with CMOS sensor, sensitive in the wavelength range 400-1000 nm. Figure 1 reports the relative camera spectral response ($S_{c,rel}$) which is the spectral response of the camera S_c, which is reported in the camera datasheet, divided by its maximum value. The peak of sensitivity is at 534 nm (visible green), but the camera is also sensible in the infrared, as shown by the superposition with the visible light spectrum.

In order to optimize the signal received by the camera CMOS sensor and filter out the light radiated by the hot steel bar; the radiation spectrum of hot forging materials is analysed.

The temperature of hot forging for open die forging is usually between 750 and 1200 °C [15].

Hot forged products, as reported in literature [9], can be regarded as blackbody, therefore when the temperature is constant the variation of blackbody spectral irradiance $B(\lambda, T)$ with wavelength conforms to the Planck law (1):

$$B(\lambda,T) = \frac{2\,h\,c^2}{\lambda^5} \cdot \frac{1}{\left(e^{\frac{h\,c}{\lambda\,k\,T}} - 1\right)} \text{ in } \frac{\mathrm{W}}{\mathrm{m^2 \cdot sr \cdot m}}, \quad (1)$$

where λ is the wavelength measured in m, T is the temperature in K and the constants are:

- c is the speed of light in vacuum, $c = 2.998 \times 10^8$ m · s^{-1}
- h is the Planck constant, $h = 6.626 \times 10^{-34}$ W · s^2
- k is the Boltzmann constant, $k = 1.381 \times 10^{-23}$ W · s · K^{-1}.

The blackbody emission model is an uncertain representation of the effective emission of the hot steel parts, mainly due to the uncertainty related to the emissivity of the body, which in this paper is not addressed. However, even using a theoretical model, the issue of laser line contrast over an incandescent body can be explained in a comprehensive way.

Figure 2 reports the spectral radiance of the blackbody spectrum calculated in the cases of temperature 1000 °C, 1100 °C and 1200 °C (both in linear Figure 2-a and logarithmic Figure 2-b scale) using Equation (1). The abscissa of the curve peak decreases with blackbody temperature increase, ranging from 2276.5 nm @1000 °C to 1967.3 nm @1200 °C which corresponds to a frequency shift of 309.2 nm. To filter out the light radiating from the blackbody, the interferential filter of the camera should therefore be a short wavelength pass filter because in the lower wavelengths of the visible spectrum the spectral radiance of the blackbody decreases.

The cut-off wavelength to be chosen for the interferential filter depends upon both the temperature of the hot steel bar and also the spectral radiance of the laser line emitter. The light

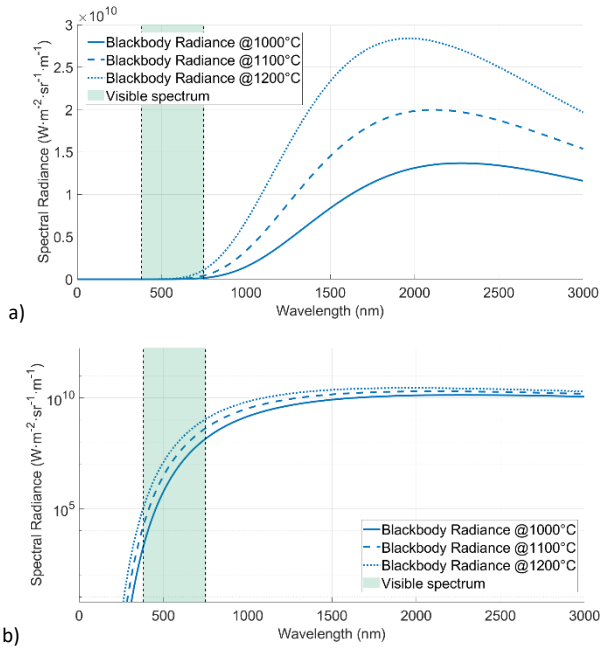

Figure 2. Blackbody spectral irradiance in a) linear and b) logarithmic scale.

radiating from the blackbody is influenced by the camera spectral response. According to Equation (2) the spectral irradiance of a blackbody under the influence of the relative response of the camera, defined as $S_{\mathrm{c-b}}$, is:

$$S_{\mathrm{c-b}}(\lambda, T) = B(\lambda, T) \cdot S_{\mathrm{c,rel}} \,. \tag{2}$$

The curves of $S_{\mathrm{c-b}}$, reported in Figure 3 show that, in the visible range, the blackbody emission that reaches the camera sensor is high with a peak at 680-700 nm considering the temperature of the emitting object between 1000-1200 °C.

Therefore, the laser wavelength to be selected to inspect an incandescent object at these temperatures should be distant from this range: selecting a laser line emitter in the visible range 380-500 nm (violet-blue) would avoid capturing the hot steel bar radiance, as in this part a minimum spectral content is coming

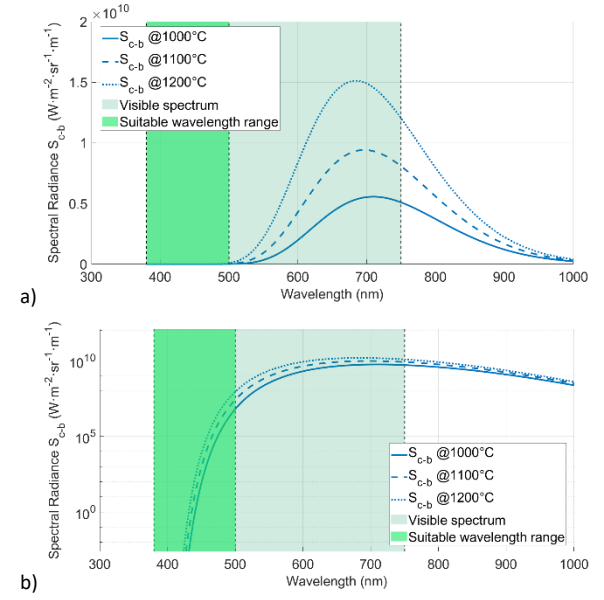

Figure 3. Blackbody spectral radiance under the influence of camera spectral response (S_{c-b}) in linear (a) and logarithmic (b) scale.

from the emitting source. For the use case application, a laser emitter at 450 nm (visible blue) has been selected. The laser plane selected for the LLT sensor is an Osela laser, model SL-450-100-RS-A-60-24V.

2.2. Design of The Laser Line Triangulation Sensor

The LLT sensor presented in this paper is designed and developed in the context of the openZDM project and features as main components an AT camera, model C5-2040-GigE, (which spectral response is reported in Figure 1) and a laser plane at 450 nm. The camera is inclined with respect to the laser plane emitter of an angle of triangulation. The system has been designed according to the requirements of the use case which are to:

- inspected different type of steel bars with average length dimension 650-1000 mm;
- detect non-straightness with an uncertainty lower than 0.2 mm (10 % of max tolerance).

The sensor has been designed to cover a large measurement range resulting in a transversal Field-Of-View (X-FOV) from 800 mm to 2000 mm and a minimum Z distance of 630 mm in the near field up to 1580 mm in the far field. This measurement range is obtained, given the geometrical configuration of the sensor, by fixing the stand-off distance (SO) of the sensor at 1000 mm with an angle of triangulation α of 45° [13].

The camera-laser distance D, which corresponds to the overall length of the sensor, results therefore to be 1000 mm given $D = SO \times \sin(\alpha)$.

The product positioning has been chosen so that the bar to be inspected is positioned around the stand-off by the robot which picks up the heated bar with a gripper on one side. The laser line is projected onto the bar on the side, as shown in Figure 4, therefore the laser line profile is extracted in the XZ plane.

The laser line wavelength from quality control report (date 28-04-2023) is assessed to be 451.8 nm therefore to enhance SNR and block out all the other spectral content from the camera, the camera optics are equipped with a very narrowband filter centered at 451.5 ± 3 nm with peak transmission of 72.1 %. This filter, even though improving SNR of the laser line, poses limitations, has it will be further discussed in the paper.

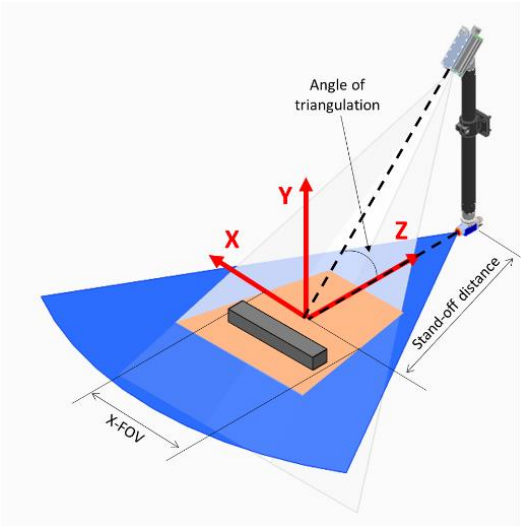

Figure 4. LLT sensor design.

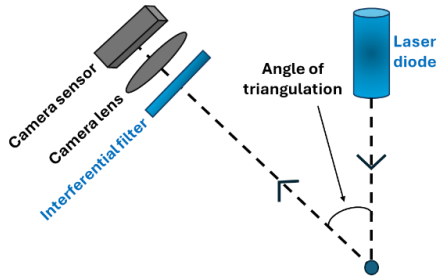

Figure 5. Laser line optical flow.

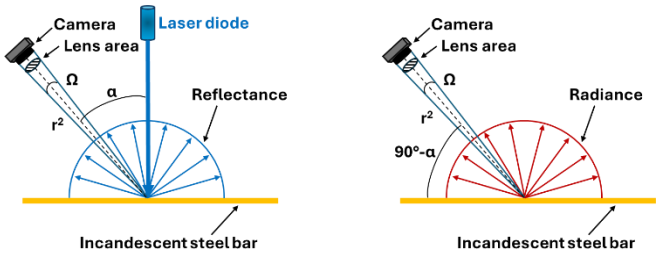

Figure 6. Signal (left) and noise (right) optical flow schema.

3. ANALYSIS OF INTERFERENTIAL FILTERS OPTICAL CHARCHTERISTICS

In this section, the optical flow of both noise and signal is described with the purpose of determining the SNR for this use case application. Different interferential filters are discussed along with the influence of the optical angle on the performances of the sensor.

3.1. Laser Line Optical Flow: Signal to Noise Ratio

The optical flow of the laser line is intercepted by an interference bandpass filter which is placed in front of the camera optics (see Figure 5).

Two different types of interferential filters are investigated:

- a very narrow band interferential filter (451.5NB3/35.5mm) centred at 451.78 nm ± 3 nm and peak transmission 72.1 %, further addressed as filter 1,
- an interference bandpass filter (MIWE Bi450-35.5) with useful Range 445-465nm ± 10 nm and peak transmission ≥ 88 %, further addressed as filter 2.

In this paragraph the Signal to Noise ratio is evaluated considering the optical flow of both noise and signal which are respectively the signal deriving from the bar irradiance and the LLT laser emitter signal. The interferential filter is placed in front of the camera optics and therefore introduces attenuation to both noise and signal. Thus, evaluating SNR is fundamental to identify which of the two interferential filters best fit the use case application.

Figure 6 reports a schema of the optical flow of both signal and noise: the laser diode light incidents the surface of the incandescent steel bar and is reflected. Part of this reflectance is captured by the camera which is inclined with respect to the laser line emitter of an angle of triangulation α which corresponds to 45° for the use case application. The camera optics describe in the space a solid angle Ω (see Figure 5) which can be calculated with the Equation (3) [16] given r the radius to the subtended to the area A

$$\Omega = \frac{A}{r^2} \text{ in sr.} \tag{3}$$

Firstly, the optical flow of the laser line signal is analysed considering the laser line power emission, the transmission functions of the filters and the camera spectral response. The filters are different in wavelength tolerance as the first filter is centred in the laser line emitter wavelength which from quality control report is 451.8 nm with the peak width of 3 nm.

Figure 7 reports the laser line signal optical flow: the laser spectral radiance is reduced due to the presence of the interferential filter and the relative camera spectral response $S_{\mathrm{c,rel}}$ (58 % quantum efficiency @450 nm, which reported in relative scale is 0.88). The laser line peak is therefore reduced both in amplitude and in width. The laser peak amplitude has an output power of 75.3 mW from quality control report. The laser line spectral radiance S_l is calculated approximating the laser line peak with a gaussian curve with ± 3 nm center wavelength tolerance, which is the usual wavelength tolerance for laser diodes. Figure 7-a reports the relative laser line spectral radiance $S_{\mathrm{l,rel}}$ calculated as in equation (4):

$$S_{\mathrm{l,rel}} = \frac{S_{\mathrm{l}}}{\max\left(S_{\mathrm{l}}\right)}. \tag{4}$$

Laser line spectral radiance is attenuated: the laser line peak value decreases to 0.64 in the case of the interference filter 1 451.5 ± 3 nm and to 0.79 in the case of the interference filter 2 450 ± 10 nm (Figure 7-d). The values of the resulting signal S (Figure 7-d) are obtained given the formula (5):

$$S = S_{\mathrm{l,rel}} \cdot S_{\mathrm{f,rel}} \cdot S_{\mathrm{c,rel}}\,. \tag{5}$$

To consider the noise emission deriving from the bar irradiance, the hot steel product to be inspected is approximated

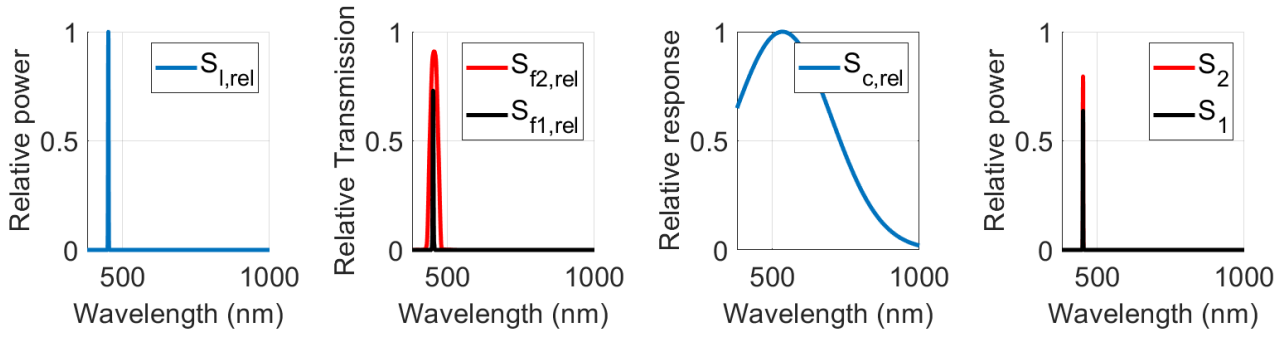

a) Initial laser spectral radiance

b) Interference filter Transmission function

c) Relative camera spectral response

d) Resulting laser spectral radiance

Figure 7. Laser line signal optical flow.

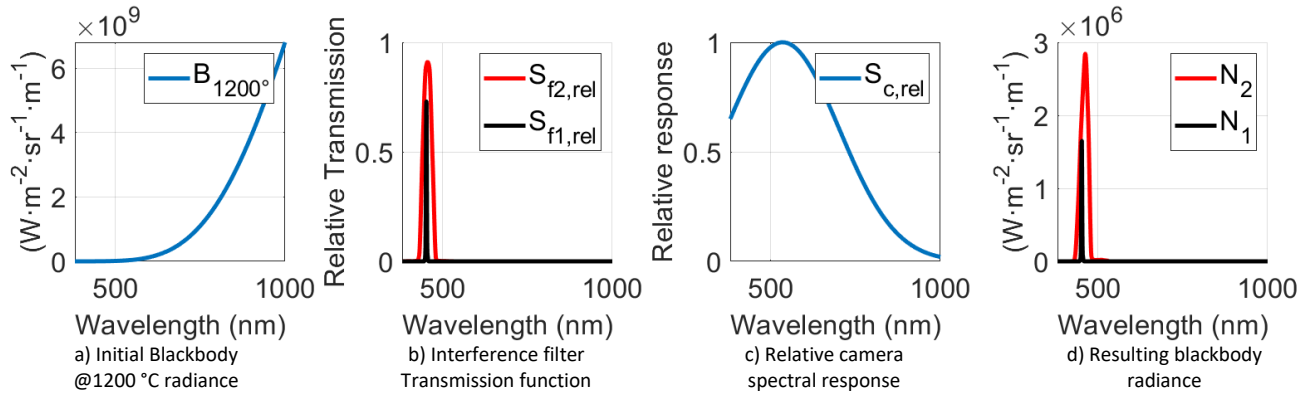

Figure 8. Noise signal optical flow.

as a blackbody @1200 °C. Figure 8-a reports the portion of the blackbody spectrum in the wavelength range 380-1000 nm. Due to the presence of the interference filter (Figure 8-b reports the filters relative transmission $S_{\mathrm{f,rel}}$), the energy radiating by the blackbody $B_{1200°C}$ is filtered and attenuated obtaining a spectral radiance N (Figure 8-d) which is calculated with the Equation (6) considering the presence of the interferential filters and the camera spectral response:

$$N = B_{1200°C} \cdot S_{\mathrm{f,rel}} \cdot S_{\mathrm{c,rel}} \cdot \tag{6}$$

Considering the very narrowband filter 1, the resulting spectral radiance reaches a peak value of 1.65×10^6 W m^{-2} sr^{-1} m^{-1} compared to the 2.83×10^6 W m^{-2} sr^{-1} m^{-1} peak value of the curve resulting from the introduction of filter 2. Therefore, noise derived from the bar irradiance is reduced in presence of the very narrowband filter.

To estimate the SNR deriving from the laser line emitter with respect to the noise of the bar irradiance, the integral of the resulting curves is calculated, considering that just the portion of spectral content subtended by the angle Ω reaches the camera sensor. The laser emitter power has been experimentally measured with an optical power meter (model 840-C Newport) resulting in 0.424 mW @1000 mm distance. The surface power density is calculated considering the laser line impacts the power meter detector on an area of 2.45×10^{-6} m^2. Indeed, the laser line emitter has a surface power density of $P_{\mathrm{d}} = 1.73 \times 10^2$ W/m^2. The camera intercepts just a portion of the laser surface power density reflected by the bar, which is proportional to $\Omega/(2 \cdot \pi)$. The solid angle Ω is calculated with Equation (3): as the camera is very far from the object of interest, $standoff = 1000$ mm, the radius r can be approximated to the radial distance of the camera to the laser spot $r \cong standoff \cdot \cos(\alpha)$, therefore $\Omega = 4.9 \times 10^{-4}$ sr $@\alpha = 45°$. The resulting surface power density, derived from the laser line reflectance, which reaches the camera sensor, is therefore $P_{\mathrm{S}} = P_{\mathrm{d}} \cdot \Omega/(2 \cdot \pi) = 1.36 \times 10^2$ W/m^2. To consider the attenuation due to the presence of the interferential filter and the camera spectral response, P_S has to be multiplied with S_1 and S_2 respectively obtaining the curves for the surface power density of the laser signal received by the camera P_{S1} and P_{S2} reported in Figure 9.

To evaluate the surface power density of the noise signal received by the camera, the spectral radiance N is multiplied by the solid angle Ω obtaining P_{N1} and P_{N2} reported in Figure 9, respectively considering the introduction of filter 1 (Figure 9-a) or filter 2 (Figure 9-b).

The camera sensor of the LLT sensor presented is a CMOS sensor [17] which means the pixel intensity derives from the incident photons on the pixel area during the integration time. Therefore, the integral of the curves for surface power density for both signal P_S and noise P_N is computed with respect to the spectral wavelength, obtaining the results reported in Table 1.

The third column of Table 1 represents a comparison between the filter 1 and filter 2. Filter 1, with respect to filter 2, attenuates both noise and signal. However, the attenuation of the signal is limited to -29 % while the attenuation of noise is significantly larger around -93 %. This allows to conclude that in presence of a very narrowband filter, as filter 1, the Signal to Noise ratio increases.

However, introducing a very narrow band filter poses other limits to the application such as that the light is highly attenuated

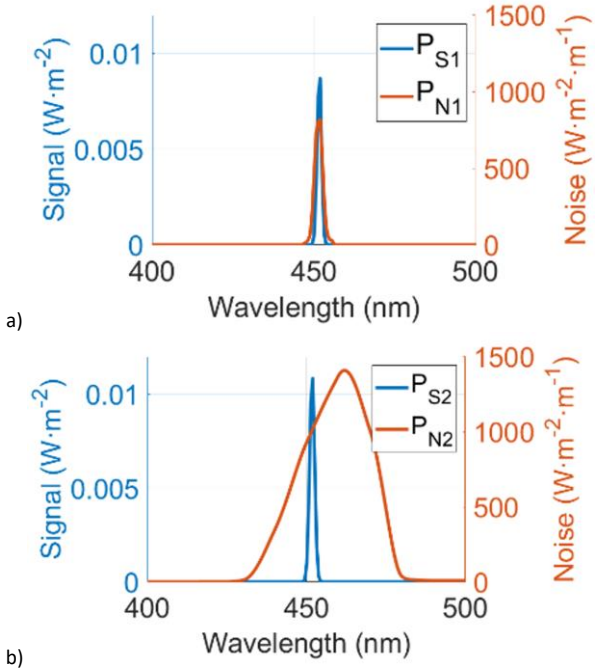

Figure 9. Signal to Noise Ratio evaluation with a) interference filter 1 at 451.8 ± 3 nm and b) interference filter 2 at 450 ± 10 nm.

Table 1. SNR evaluation results.

	Filter 1	Filter 2	Comparison Filter1-2
Signal	1.51×10^{-11} W·m^{-1}	2.14×10^{-11} W·m^{-1}	-29 %
Noise	2.64×10^{-6} W·m^{-2}	3.75×10^{-5} W·m^{-2}	-93 %

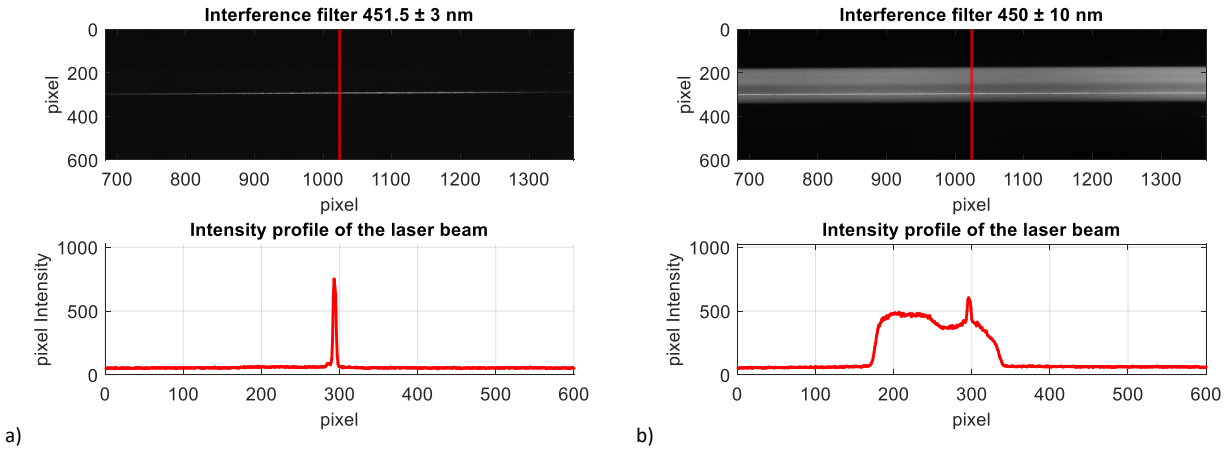

Figure 10. Image of incandescent steel bar (top) and corresponding pixel intensity curve extracted on the red line (bottom) with a) interference filter 1 at 451.8 ± 3 nm and b) interference filter 2 at 450 ± 10 nm.

at the edges of the field of view. This issue is discussed in paragraph 3.3 from a methodological point of view and addressed in paragraph 3.4 referring to the use case application.

3.2. Steel Bar Use Case Signal to Noise Ratio Evaluation

Considering the use case of the measurement of a hot steel bar with the laser line triangulation sensor, the SNR has been evaluated with both the interferential filters presented: filter 1 451.8 ± 3 nm and filter 2 at 450 ± 10 nm. The interferential filter 2 does not block all the spectral content coming from the bar irradiance, indeed there is a pedestal of high pixel intensity value which corresponds to the top part of the bar (see Figure 10-b bottom). In this case the SNR is very low, just 2 dB given the peak of the laser line which is at 604 pixel intensity while the pedestal at 480 pixel intensity. On the other hand, using a very narrow band filter such as filter 1 increases the SNR exponentially reaching 21.94 dB given the peak is at pixel intensity 750 and the background at 60 (see Figure 10-a bottom). Moreover, the whole spectral content coming from the bar irradiance is removed and the laser line peak is sharp and easily detectable as no other peaks are present. Therefore, this filter should be preferred in order to obtain good image quality and therefore a precise measurement, as the laser line peak position is clearly identifiable by the Laser Line Extraction algorithms.

However, using a very narrow band filter can pose limits in terms of optical angle and X-FOV which can be reduced with respect to the nominal values at the edges of the filter where the transmission of the interferential filter decreases. These issues will be addressed in the following paragraphs.

3.3. Optical Angle Sensitivity

The optical characteristics of interference filters depends on the thickness of the film [18] therefore changing the angle of laser line incidence, the characteristic of the filter will change: increasing the angle of light incidence, light passes obliquely through the filter and its optical path increases. This implies a change in the filter optical characteristics which, for moderate angles, results in a shift to a shorter wavelength. The wavelength shift with obliquity is approximated by the Equation (7).

$$\lambda_\theta = \frac{\lambda_0}{n}\sqrt{n^2 - \sin^2\theta}\,, \tag{7}$$

where λ_θ is the shifted wavelength at an angle of incidence θ, λ_0 is the wavelength for normal incidence and n is the "effective index" for the thin film which typically ranges from 1.5 to 1.9 for most coatings.

The shifted wavelength is calculated considering the laser line emitter nominal wavelength 451.8 nm (from quality control report) with its upper and lower limits. Given the ranges of the two interferential filters selected from the curves of the laser line emitter wavelength shift (Figure 11-b) it is visible that the laser line is filtered out by the thin film if the incident laser light angle exceeds 15.6° and 35.1° respectively with filter 1 – interference filter 451.8 ± 3 nm – and filter 2 - interference filter 450 ± 10 nm. The laser nominal wavelength itself can shift ± 3 nm given the laser diode tolerance reported in literature [19], which is highlighted by the two blue dashed curves in Figure 11-b.

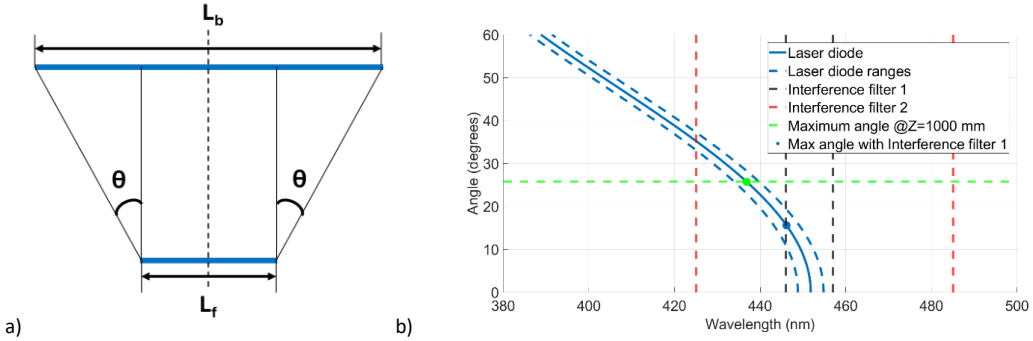

Figure 11. a) Schema of bar-filter position and b) interferential filter wavelength shift given filter 1 – interference filter 451.8 ± 3 nm – and filter 2 - interference filter 450 ± 10 nm.

The laser line triangulation sensor has been designed with a standoff distance of 1000 mm along the Z axis while the maximum bar length along the X axis is L_b = 1000 mm. Considering that the filter has a diameter length L_f = 35.5 mm, the maximum angle of inclination $\vartheta_{\max}$ @Z = 1000 mm can be calculated with the Equation (8), given the schema reported in Figure 11-a:

$$\vartheta_{\max} = \arctan\left(\frac{(L_b - L_f)/2}{Z}\right). \quad (8)$$

Given these conditions $\vartheta_{\max} = 25.75°$ which is represented by the green dashed line in Figure 11-b. The intercept between this line and the blue curve is highlighted with a green point: with $\vartheta_{\max}$ as inclination angle, the wavelength shift corresponds to about 437 nm which is included in the tolerance ranges of filter 2 but not in the ranges of filter 1. This means that filter 1, which is a very narrowband filter, does not allow to properly frame all L_b at the standoff distance but portion of the bar where the laser line is projected gets filtered out. The issue is now to calculate, for this Z distance, the maximum length of the bar which can be framed with filter 1, which is surely below 1000 mm. Given filter1, the maximum angle which is allowed so that the laser line reflection remains in the filter ranges, considering the wavelength shift, is 15.6 ° (blue point in Figure 11-b), which corresponds to the intercept between the blue curve of the laser line diode and the dashed black line of lower limit of the interference filter 1. Considering this as $\vartheta_{\max}$ and inverting Equation (8) to calculate L_b @Z = 1000 mm, the result is 669 mm. This means that a bar long 1000 mm is not measurable because about 330 mm at the edges are left out (165 mm at each edge respectively) which corresponds to 33 % of the bar length.

3.4. Interference Filters Application to Steel Bar Use Case

A reference ruler of 1 m length has been selected to validate the performance of the laser line triangulation sensor at ambient temperature. Figure 12 reports two raw images of a reference ruler of a 1000 mm length, Figure 12-a with the filter 1 installed in the camera while Figure 12-b with filter 2.

From the images it is evident that the interference filter 1 is so narrowband that some part of the ruler edges is filtered out. Figure 13 reports the result of the measurement which are the extracted laser line profiles. The reference system XZ adopted is the one of the laser line triangulation sensor (see reference system in Figure 4). The bar positioning is not the same as the measurements have been performed manually positioning the component for inspection. Thus, there is a different Z distance between ruler and laser line emitter: for ruler with filter 1

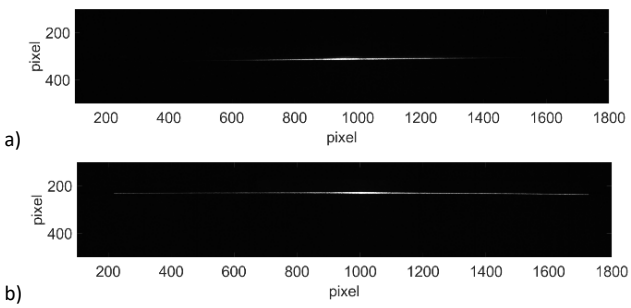

Figure 12. Image of a reference ruler acquired at ambient temperature with a) filter 1 – interference filter 451.8 ± 3 nm – and b) filter 2 - interference filter 450 ± 10 nm.

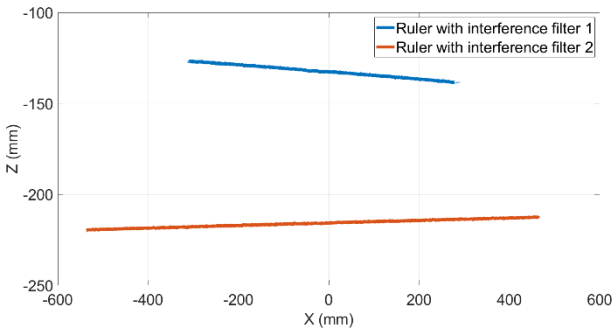

Figure 13. Laser line profile of a reference ruler with filter 1 – interference filter 451.8 ± 3 nm – and filter 2 - interference filter 450 ± 10 nm.

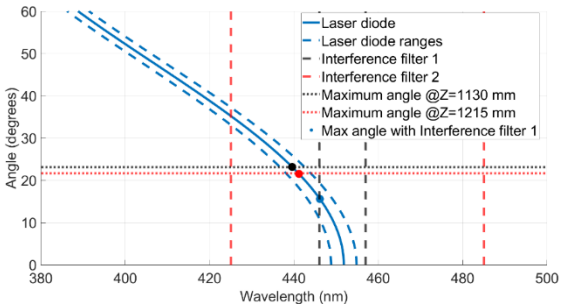

Figure 14. interferential filter wavelength shift and maximum inclination angle admissible for filter 1 – interference filter 451.8 ± 3 nm – and filter 2 - interference filter 450 ± 10 nm.

$Z \simeq$ -130 mm which corresponds to 1130 mm laser-ruler distance, while for ruler with filter 2 $Z \simeq$ -215 mm which corresponds to 1215 mm laser-ruler distance.

Considering filter 1, the maximum inclination angle admitted for 1000 mm @Z = 1130 mm is 23° which, referring to Figure 14, corresponds to a point where the laser line wavelength shift is surely outside the filter 1 tolerances. At this distance Z = 1130 mm, the length of the bar allowed L_b, given the $\vartheta_{\max}$=16° (see blue point in Figure 14) is 665 mm.

From the measurement taken at ambient temperature of ruler with filter 1, the length of the ruler is 587 mm. With respect to the maximum L_b allowed of 665 mm the results are in the same order of magnitude; this difference is expected because the ruler is not accurately centred in the X-FOV and the optical properties at the edges of the lens degrade more which has not been taken into account in the theoretical modelling of the optical flow (Section 2).

On the other hand, measurement taken with filter 2 on the reference ruler show a 1000 mm length measurement; instead, measurement taken with filter 1 underestimates the bar length. Given L_b=1000 mm, the Equation (8) result $\vartheta_{\max} = 22°$ @Z = 1215 mm (red point in Figure 14) which is in fact included in the admittible range for interference filter 2, given the wavelength shift of the laser line diode.

4. OPTICAL OPTIMIZATION METHODOLOGY FOR INLINE APPLICATION

This section discusses the methodology to optimize the laser line acquisition considering both optical acquisition parameters and Laser Line Extraction (LLE) algorithms.

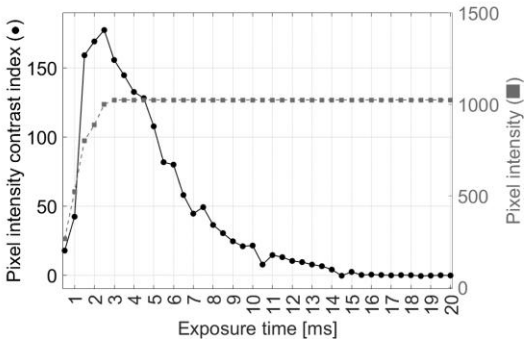

Figure 15. Image intensity and contrast dependence to exposure time.

4.1. Optical Acquisition Settings Optimization

In the inline application of the steel industry, the laser line has a pixel intensity comparable to the one of the bar, due to the bar emission condition and angular position of the camera with respect to the bar geometry. Therefore, it is fundamental to achieve an optimal setting of the acquisition parameters to maximize the contrast of the laser line with respect to the metal surface of the object to be measured. Different approaches can be used such as the implementation of machine learning or threshold-based algorithms [20]. To optimize the acquisition settings for incandescent steel bars images, a parametric analysis has been performed on the exposure time which widely impacts on the contrast of the laser line with respect to the background. It is shown that an exposure time of 2.5 ms optimizes the contrast between the laser line pixel intensity with respect to the one of pixel intensity of the bar (see Figure 15) thus improving the overall laser line SNR. The pixel intensity contrast index is computed identifying the maximum value of pixel intensity, for each pixel column 1÷2048, in the portion of the bar above the laser line (from pixel row 180 to 240, see Figure 16-a) and in the portion of the image with the laser line (from pixel row 280 to 315, see Figure 16-b, region in gray). The pixel intensity contrast index (reported in Figure 15 on the left ordinate axis) is then identified averaging the difference between these two maxima for each pixel column, considering just the pixel columns with presence of the bar in region 510÷1700 pixel). From 3 ms exposure time on, the maximum pixel intensity value of the image (curve reported in Figure 15 on the right ordinate axis), which corresponds to the laser line, reaches saturation (1023 is maximum pixel intensity given 10-bit image format), therefore contrast between laser line and bar intensity decreases.

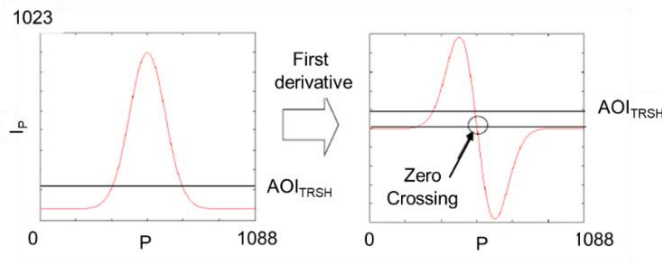

Figure 17. Camera embedded FIR Peak Laser Line Extraction Algorithm [21].

Exposure time has therefore been set to 2.5 ms and both raw images and extracted laser line profiles of the hot bar have been acquired (see Figure 16). However, data have shown that, even fine-tuning others optical parameters, the laser line peak is not clearly detectable by the algorithm and gets confused with the background of the incandescent steel bar because the peak pixel intensity is less than 2 dB higher (see Figure 16-b).

4.2. Software Optimization for Laser Line Extraction

In the case of framing an incandescent bar the Signal to Noise Ratio is critical and the camera embedded laser line extraction algorithm finds difficulty in properly identifying the laser line. The laser line triangulation sensor features a smart camera, model AT C5 2040GigE [21], which can be used both as a 2D camera acquiring grayscale images but also in 3D mode. This functionality enables for direct identification of the laser line thanks to the implementation of embedded laser line extraction algorithms, therefore the camera outputs directly the laser line position array. Different types of algorithms have been developed for laser line extraction, the most common are maximum peak, threshold, but in literature other algorithms have been investigated for example improved grayscale centre of gravity [22] or deep Learning Skeleton Extraction Network [23]. In this case the FIR Peak algorithm is implemented [24] which firstly calculates the first derivative of the laser beam profile with Finite Impulse Response filter (FIR), then defines the laser line profile position as the zero-crossing point. The AOI_{TRSH} is used to detect the first rising edge of the derived intensity signal (see Figure 17).

Figure 16 reports a measurement taken in production line of a steel bar: Figure 16-a is the image of the steel bar, Figure 16-b is the pixel intensity profile along the column 1024 of the image (white vertical line highlighted in Figure 16-a) and Figure 16-c corresponds to the laser line profile extracted. As it can be seen from Figure 16-b the peak which corresponds to the laser line, which is around row 300 of the image, is not preponderant with

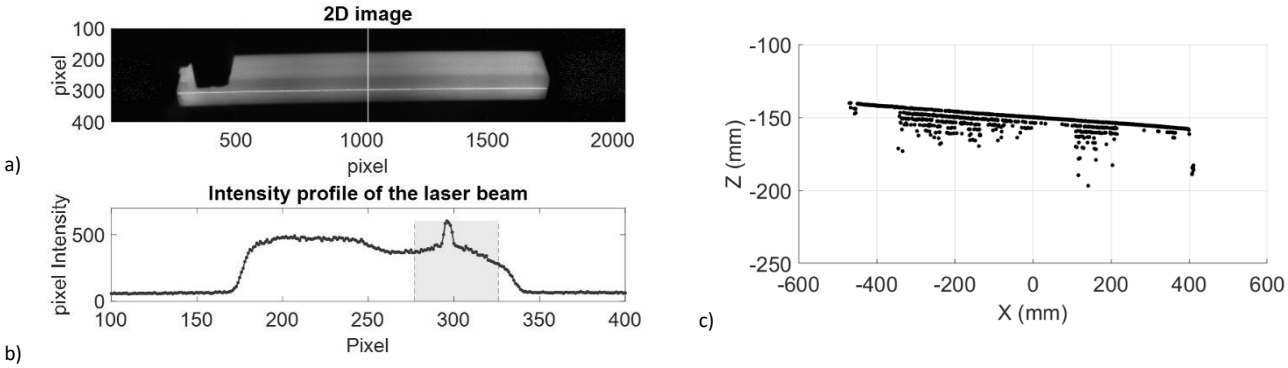

Figure 16. a) Raw Image of incandescent bar, b) pixel intensity profile along column 1024 of the image (highlighted with white vertical line in the image) and c) correspondent laser line profile extracted.

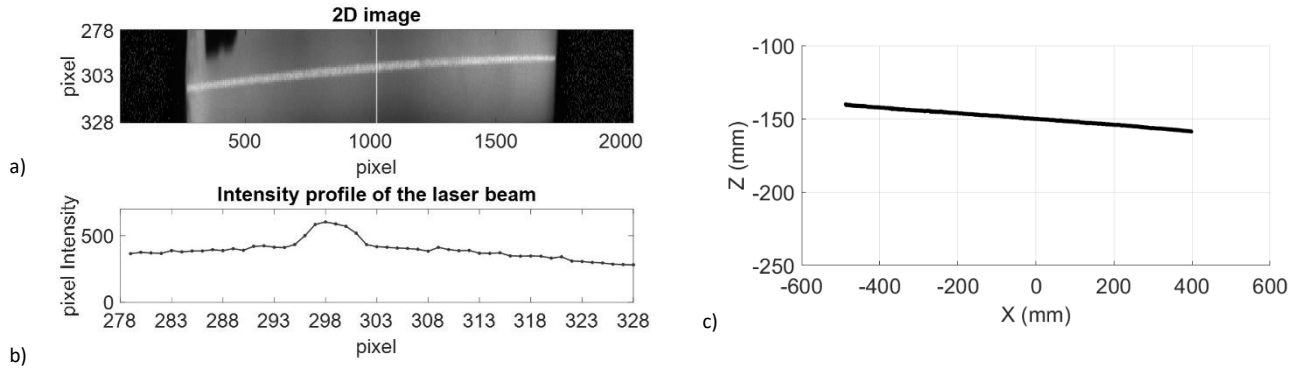

Figure 18. a) Region of Interest of raw Image of incandescent bar, b) pixel intensity profile along column 1024 of the image (highlighted with white vertical line in the image) and c) correspondent laser line profile extracted (c) with ROI introduction.

respect to the rest of the image as there is a pedestal corresponding to the high pixel intensity of the incandescent steel bar. When applying the laser line extraction algorithm, and

calculating the derivative of the curve, the first rising edge of the pedestal of the pixel intensity is mismatched with the peak of the laser line, leading to many outliers and therefore a noisy measurement (see Figure 16-c).

To solve this issue, the methodology proposed is the preprocessing of the image with the introduction of a ROI of 50 pixels height around the laser line which both reduces data storage but most of all allows to obtain a pixel intensity profile with just one peak, which is therefore clearly identified by the algorithm as the laser line (Figure 18-c).

4.3. Laser line estimation uncertainty

The laser line is determined by a linear interpolation of the scattered data representing the laser line peaks. The amount of scatter of these data is an estimate of the uncertainty of this linear regression. Therefore, we estimate the residuals of the linear interpolation, by computing their RMS dispersion.

Before the introduction of the ROI (Figure 16-c), this dispersion amounts at 4.9 while, after the introduction of the ROI (Figure 18-c), the dispersion of the residuals reduces significantly to 0.2.

Therefore, the introduction of the ROI has produced a significant improvement in the scatter of laser line peak data and in the corresponding quality of the linear regression. Moreover, the ROI introduction enables an outliers reduction of 97.5 % with respect to the case without ROI introduction Therefore, the methodology has produced a significant improvement in uncertainty of laser line extraction.

However, this solution imposes the constraint of a repeatable positioning of the product in the measurement range as otherwise the laser line would fall out of the ROI. Given that the camera has 1088 pixel rows and the Z range is 950 mm, the available region for product positioning is about 43 mm. This imposes a constraint in the product positioning tolerance which has to be respected by the robot in charge of product handling.

5. CONCLUSIONS

The methodology presented has highlighted the challenges and limits of using a laser line triangulation sensor for geometry measurement of an incandescent steel object showing that, in case of a very narrow band interferential filter, noise coming from the bar irradiance is reduced by 93 % with respect to the introduction of an interferential filter with a greater wavelength tolerance. The results regarding the inline application on an incandescent steel bar have shown coherence with respect to the methodology presented proving that, even though the very narrowband filter increases SNR, the signal at edges of the field of view is very attenuated due to the laser line wavelength shift which depends on the incident optical angle.

A measurement taken at ambient temperature on a reference ruler has shown that 40.3 % of the length of the bar is not detected with respect to the measurement without the very narrow band filter. Even though increasing the laser-object distance can be a solution, as the X-FOV increases, this is not always feasible due to constraint of the production plant. Therefore, a software methodology to enhance SNR has been described introducing a Region of Interest on the image which enables for correct laser line extraction also in critical optical conditions, as the laser line peak is just 2 dB than the bar pixel intensity. This solution reduces the uncertainty of the laser line extraction as the RMS dispersion of the residuals decreases significantly from 4.9 to 0.2. The introduction of a fixed region of interest poses however the limit to the product positioning in a region of tolerance of 43 mm which has to be respected by the robot gripper. Future development of the work could be implementing a different kind of laser line extraction algorithm which can overcome the limits of the ROI approach or introducing another camera which is more spectral selective to the laser line wavelength.

ACKNOWLEDGEMENT

This work was partially supported by OPENZDM project. This is a project from the European Union's Horizon Europe research and innovation program under Grant Agreement No. 101058673 in the call HORIZON-CL4-2021-TWIN-TRANSITION-01.

REFERENCES

[1] openZDM project, Website. Online [Accessed 01 January 2025] https://www.openzdm.eu/

[2] X. Wen, J. Wang, G. Zhang, L. Niu, Three-Dimensional Morphology and Size Measurement of High-Temperature Metal Components Based on Machine Vision Technology: A Review. Sensors, 2021, 21(14), 4680. DOI: 10.3390/s21144680

[3] S. Pasinetti, G. Sansoni, F. Docchio, In-Line Monitoring of Laser Welding Using a Smart Vision System, Workshop on Metrology for Industry 4.0 and IoT, Brescia, Italy, 16-18 April 2018, pp. 134-

139.
DOI: 10.1109/METROI4.2018.8428332

[4] R. Schmitt, T. Pfeifer, G. Mallmann, Machine integrated telecentric surface metrology in laser structuring systems, Acta IMEKO 2 (2) 2013, pp. 73-77.
DOI: 10.21014/acta_imeko.v2i2.106

[5] A. Bernieri, L. Ferrigno, M. Laracca, A. Rasile, M. Ricci, Ultrasonic non destructive testing on aluminium forged bars, 2017 IEEE Int. Workshop on Metrology for AeroSpace (MetroAeroSpace), Padua, Italy, 21-23 June 2017, pp. 223-227.
DOI: 10.1109/MetroAeroSpace.2017.7999569

[6] S. B. Dworkin, T. J. Nye, Image processing for machine vision measurement of hot formed parts, Journal of Materials Processing Technology, Volume 174, Issues 1–3, 2006, pp. 1-6.
DOI: 10.1016/j.jmatprotec.2004.10.019

[7] H.-l. Yu, K. Tieu, C. Lu, G.-y. Deng, X.-h. Liu, Occurrence of surface defects on strips during hot rolling process by FEM, The Int. Journal of Advanced Manufacturing Technology, Volume 67, pp. 1161–1170.
DOI: 10.1007/s00170-012-4556-7

[8] D. Bračun, G. Škulj, M. Kadiš, Spectral selective and difference imaging laser triangulation measurement system for on line measurement of large hot workpieces in precision open die forging, Int. J. Adv. Manuf. Technol. 90 (1–4), 2017, pp. 917–926.
DOI: 10.1007/s00170-016-9460-0

[9] Z. Jia, B. Wang, W. Liu, Y. Sun, An improved image acquiring method for machine vision measurement of hot formed parts, J. Mater. Process. Technol. 210 (2) 2010, pp. 267–271.
DOI: 10.1016/j.jmatprotec.2009.09.009

[10] K. Määttä, J. Kostamovaara, R. Myllylä, Measurement of hot surfaces by pulsed time-of-flight laser radar techniques, Proc. of SPIE, vol. 1265, Industrial inspection II, 12–13 Mar 1990, pp. 179–191.
DOI: 10.1117/12.20246

[11] K. Määttä, J. Kostamovaara, R. Myllylä, A laser rangefinder for hot surface profiling measurements, Proc. of SPIE, vol. 952, Laser Technologies in Industry, pp. 356–364.
DOI: 10.1117/12.968857

[12] B. Wang, A study on length measurement method of hot large forgings based on binocular vision system, Measurement 199 (2022), 111586.
DOI: 10.1016/j.measurement.2022.111586

[13] V. Pasquinelli, M. Martarelli, N. Paone, (+ another 6 authors), Beam Straightness Measurement with Laser Triangulation System: a steel industry use case, 2023 IEEE Int. Workshop on Metrology for Industry 4.0 & IoT (MetroInd4.0&IoT), Brescia, Italy, 6-8 June 2023, pp. 130-135.
DOI: 10.1109/MetroInd4.0IoT57462.2023.10180023

[14] Aneta Zatočilová, David Paloušek, Jan Brandejs, Image-based measurement of the dimensions and of the axis straightness of hot forgings, Measurement, Volume 94, 2016, pp. 254-264.
DOI: 10.1016/j.measurement.2016.07.066

[15] Lv Y (1995) Forging technology. China Machine Press, Beijing, pp 20

[16] Orin Packer, David R. Williams, 2 - Light, the Retinal Image, and Photoreceptors, Editor(s): Steven K. Shevell, The Science of Color (Second Edition), Elsevier Science Ltd, 2003, pp. 41-102.
DOI: 10.1016/B978-044451251-2/50003-9

[17] M. Bigas, E. Cabruja, J. Forest, J. Salvi, Review of CMOS image sensors, Microelectronics Journal, Volume 37, Issue 5, 2006, pp. 433-451.
DOI: 10.1016/j.mejo.2005.07.002

[18] Warren J. Smith's, Modern Optical Engineering: The Design of Optical Systems, McGraw-Hill, 2000, 0071363602

[19] Photonics Handbook. Online [Accessed 01 January 2025] https://www.photonics.com/Articles/Laser_Diodes_Specification_Guidelines/p4/a25157

[20] D. Di Gasbarro, G. D'Emilia, E. Natale, Optical system for on-line monitoring of welding: A machine learning approach for optimal set up, Acta IMEKO, vol. 5, issue 4, 2016, pp. 4-11.
DOI: 10.21014/acta_imeko.v5i4.420.

[21] Automation Technology, AT Camera C5-2040-GigE Manual. Online [Accessed 10 January 2025] https://ftp.stemmer-imaging.com/webdavs/docmanager/117760-Automation-Technology-User-Manual-C5-Series.pdf

[22] R. Yao, B. Wang, M. Hu, D. Hua, L. Wu, H. Lu, X. Liu, A Method for Extracting a Laser Center Line Based on an Improved Grayscale Center of Gravity Method: Application on the 3D Reconstruction of Battery Film Defects, Applied Sciences. 13, 2023. 9831.
DOI: 10.3390/app13179831

[23] S. Luo, K. Yang, L. Yang, Y. Wang, X. Gao, T. Jiang, C. Li, Laser Curve Extraction of Wheelset Based on Deep Learning Skeleton Extraction Network. Sensors 2022 Jan 23, 22(3), 859.
DOI: 10.3390/s22030859

[24] V. Pasquinelli, M. Martarelli, N. Paone, W. van de Kamp, B. Verhoef, Laser Line Triangulation Sensor with Wide Measurement Range: a Steel Industry Use Case, 2024 IEEE Int. Workshop on Metrology for Industry 4.0 & IoT (MetroInd4.0 & IoT), Firenze, Italy, 29-31 May 2024, pp. 470-475.
DOI: 10.1109/MetroInd4.0IoT61288.2024.10584183